Palaeoenvironmental response of mid-latitudinal wetlands to PETM climate change (Schöningen lignite deposits, Germany)

Katharina Methner[1], Olaf Lenz[2], Walter Riegel[2], Volker Wilde[2], Andreas Mulch[1,3]

[1]Senckenberg Biodiversity and Climate Research Centre, Frankfurt am Main, 60325, Germany
5 [2]Senckenberg Research Institute and Natural History Museum Frankfurt, Frankfurt am Main, 60325, Germany
[3]Institute of Geosciences, Goethe University Frankfurt, Frankfurt am Main, 60438, Germany

Correspondence to: Katharina Methner (katharina.methner@senckenberg.de)

Abstract. The Paleocene-Eocene Thermal Maximum (PETM) offers insight into massive short-term carbon cycle perturbations that caused significant warming during a high-pCO_2 world, affecting both marine and terrestrial ecosystems.
10 PETM records from the marine-terrestrial interface (e.g. estuarine swamps and mire deposits) are, therefore, of great interest as their present-day counterparts are highly vulnerable to future climate and sea level change. Here, we assess paleoenvironmental changes of mid-latitudinal Late Paleocene-Early Eocene peat mire records along the paleo-North Sea coast. We provide carbon isotope data of bulk organic matter ($\delta^{13}C_{TOC}$), organic carbon content (%TOC), and palynological data from an extensive peat mire deposited at a mid-latitudinal (ca. 41 °N) coastal site (Schöningen, Germany). The $\delta^{13}C_{TOC}$
15 data show a carbon isotope excursion (CIE) of -1.7 ‰ coeval with a conspicuous *Apectodinium* acme, calling for the presence of the PETM in this coastal section. Due to the exceptionally large stratigraphic thickness of the PETM at Schöningen (10 m of section) we established a detailed palynological record that indicates only minor changes in paleovegetation leading to and during the PETM. Instead, paleovegetation changes mostly follow natural successions in response to changes along the marine-terrestrial interface. Compared to other available peat mire records (Cobham, UK;
20 Vasterival, France) it appears that wetland deposits around the Paleogene North Sea have a typical CIE magnitude of ca. -1.3 ‰ in $\delta^{13}C_{TOC}$. Moreover, the Schöningen record shares major characteristics with the Cobham Lignite, including evidence for increased fire activity prior to the PETM, minor PETM-related plant species changes, a reduced CIE in $\delta^{13}C_{TOC}$, and drowning of the mire (marine ingressions) during much of the PETM. This suggests that paleoenvironmental conditions during the Late Paleocene-Early Eocene, including the PETM, consistently affected major segments of the paleo-North Sea
25 coast.

1 Introduction

Among the early Cenozoic climate perturbations, the Paleocene-Eocene Thermal Maximum (PETM) at ~56 Ma (McInerney and Wing, 2011) is one of the best-investigated Cenozoic hyperthermals. Being first described in marine deposits (Kennett and Stott, 1991), the PETM has soon been recognized as a global event, equally detectable in continental environments (e.g.

5   Bowen et al., 2015; Koch et al., 1992; Magioncalda et al., 2004). However, despite the many globally distributed records, there is still debate about the cause and feedbacks of this hyperthermal (see review of McInerney and Wing, 2011). Due to the massive carbon input into the ocean-atmosphere system, global warming of 5-10°C during the PETM was associated with a distinct negative shift in carbon isotope records (δ^{13}C) (e.g. Dunkley Jones et al., 2013; McInerney and Wing, 2011; Sluijs et al., 2006, 2011; Sluijs and Dickens, 2012; Zachos et al., 2003). This negative carbon isotope excursion (CIE) is well

10   recognized in a variety of different materials from various settings. In general, the PETM CIE consists of a rapid onset, the main body of the excursion and a two-step recovery composed of an early rapid phase followed by a more gradual increase in δ^{13}C values (McInerney and Wing, 2011).

Despite this general pattern, the magnitude of the CIE varies largely between different environmental settings (on av. -2.5 to -5.5‰) and within individual records (-0.6 to -8.0‰) (see compilation of McInerney and Wing, 2011). The CIE is typically

15   larger in continental (with a mean of 4.7±1.5‰ when compared to marine depositional environments. Multiple hypotheses exist to explain the ^{13}C-depleted carbon input to the atmosphere-ocean system causing the CIE, including methane clathrate destabilization on shelfs (Dickens et al., 1995), thermogenic methane formation by magma injections into organic-rich mudstones (Svensen et al., 2004), oxidation of vast amounts of organic matter by drying of epicontinental seas (Higgins and Schrag, 2006), orbitally triggered permafrost thawing (DeConto et al., 2012), or wildfires and burning of peatlands (Kurtz et

20   al., 2003) potentially triggered by a meteorite impact (Cramer and Kent, 2005; Kent et al., 2003). In all cases, the magnitude of the CIE potentially reveals (via mass balancing) the source of carbon input to the ocean-atmosphere system. The variable preservation of the CIE in terms of magnitude and duration in different archives (Trampush and Hajek, 2017), however, provides challenges evaluating the carbon source and carbon release mechanisms (e.g. Lyons et al., 2019).

Assessing duration and magnitude of the CIE and from the related PETM warming at the marine-terrestrial interface is of

25   great interest, as near coastal ecosystems are especially vulnerable to global climate change and sea level rise causing large ecological and economic threats (IPCC, 2014). Near-coastal wetlands play a major role in the global carbon cycle as important organic carbon sinks (e.g. Raghoebarsing et al., 2005; Rumpel et al., 2018), but simultaneously are a primary source of methane emissions to the atmosphere (Christensen et al., 2003; Kirschke et al., 2013). Peatland conservation has thus become one of the pressing tasks to meet the Paris Agreement (Rumpel et al., 2018) as under global warming peatlands

30   are likely to contribute significantly to future CO_2 emissions (e.g. Dorrepaal et al., 2009; Rumpel et al., 2018) and likely have done so during the PETM (Pancost et al., 2007). Extensive wetlands with peat forming mires and swamps were widespread in the European realm during the Cenozoic (today they are forming major economic lignite and coal deposits in

Central Europe) and may have significantly contributed to Cenozoic climate evolution on a global scale (e.g. Kurtz et al., 2003; Pancost et al., 2007).

The Schöningen opencast mine (Northern Germany) has been selected as the type locality of the Schöningen Formation (Riegel et al., 2012) and offers the opportunity to study Paleocene-Eocene climate change in wetland deposits along the

5 paleo-North Sea coast (Fig. 1a) (Riegel et al., 2012). The Schöningen Formation is mainly early Eocene in age but probably includes the topmost part of the Paleocene. It comprises ~150m of alternating lignite seams and clastic interbeds (Fig. 1b) (Brandes et al., 2012; Osman et al., 2013; Riegel et al., 2012). It has been speculated that the lower part of the Schöningen Formation covers the PETM as the shallow marine deposits of Interbed 2 exhibit a conspicuous peak in the abundance of the dinoflagellate cyst *Apectodinium* (Riegel et al., 2012). The occurrence of such high abundances of *Apectodinium* in mid- to

10 high-latitudinal sediments (Schöningen paleolatitude is ~41°N (van Hinsbergen et al., 2015); see also Supplementary Information table S1) has been proven to be indicative of the PETM (Bujak and Brinkhuis, 1998; Crouch et al., 2001; Heilmann-Clausen et al., 1985; Iakovleva et al., 2001; Sluijs and Brinkhuis, 2009; Sluijs et al., 2006, 2007). Other age constraints of the Schöningen Formation are restricted to dinocyst assemblages and scattered radiometric ages derived from the near-by Emmerstadt drill core that have been correlated to the Schöningen lignite seams. These correlations, however,

15 placed the PETM within or below the Main Seam (dinocyst zone D5nb (~54.8-54.4 Ma) occurring slightly above the basal Main Seam) (Ahrendt et al., 1995; Köthe, 2003).

To investigate if the *Apectodinium* acme in Interbed 2 is related to the PETM we studied carbon isotope ratios of bulk organic matter ($\delta^{13}C_{TOC}$) from the lower part of the Schöningen Formation (Seam 1 to Seam 2). We evaluate the corresponding palynological record to assess the paleoenvironmental evolution of this wetland and compare our geochemical

20 results to lignite records along the paleo-North Sea (Cobham, UK; Vasterival, F). Collectively, these data show a consistent CIE and uniform paleoenvironmental changes within European mid-latitudinal lignite deposits.

2 Material and methods

2.1 Study site and sampling

Active lignite mining (1978-2016) yielded excellent exposures in the now-abandoned opencast mines at Schöningen (Fig.

25 1a, Supplementary Information S1 and Fig. S1). This allowed for dense sampling of the Paleocene-Eocene Schöningen Formation (Fig. 1b) of the western rim syncline of the NW-SE trending Helmstedt-Staßfurt salt wall. From the >4000 samples, collected from more than 50 individual sections over ~30 years accompanying the mining activities in Schöningen-Südfeld, we selected 121 samples from two of the lower lignite seams (Seam 1 and Seam 2) and the corresponding clastic interbed, presumably covering the latest Paleocene and early Eocene, for isotopic analyses. The ca. 16 m record consists of

30 three individual sections recovered laterally within 50 m. Stratigraphic continuation could be ensured by the well exposed, undisturbed and laterally traceable lignite seams (e.g. Riegel et al., 2012). In order to get a more comprehensive picture of

environmental and vegetation change in the latest Paleocene/early Eocene, samples from the underlying sediments (Main Seam and Interbed 1) are included in our palynological analyses.

The lower three seams (Main Seam, Seam 1 and 2 in Fig. 1b) resemble each other in their petrographic and palynological characteristics. In general, the lignite seams are composed of an alternation of dark and medium brown layers, which often

5   have tree stumps at their base and layers or lenses of charcoal with tissue preservation in the coal matrix (Riegel et al., 2012; Robson et al., 2015). Silts to medium grained sands dominate the clastic interbeds. There is still debate about prevailing deposition conditions of the clastic interbeds (Osman et al., 2013; Riegel et al., 2012). Whereas Interbed 1 shows little evidence for fully marine conditions and rather indicates local emergence (occurrence of drift wood and rooting), Interbed 2, containing rich dinocyst assemblages with peak abundances of *Apectodinium homomorphum* and other *Apectodinium* species

10   (Fig. S4), is indicative of shallow marine depositional conditions (Riegel et al., 2012). For a more detailed description of the lithology of the sampled sections, the reader is referred to (Riegel and Wilde, 2016; Riegel et al., 2012) as well as to the detailed logs in the appendix (text S1, Fig. S1).

2.2 Carbon isotope analyses

121 samples were selected for analysis of total organic carbon content (%TOC) and carbon isotope composition of bulk

15   organic matter ($\delta^{13}C_{TOC}$), providing a %TOC and $\delta^{13}C_{TOC}$ record of 16 m with average sample spacing of ~13 cm. Sample preparation included freeze drying, grinding, removal of inorganic carbon (using 10 % HCl for 24h at 40°C), centrifugation (4x at 2800 to 3000 rpm for 4 to 8 min) and sample drying (24h at 40°C). About ~0.2 mg (lignite samples) and up to ~6 mg (marine interbed samples) were analyzed using a Flash EA 1112 (Thermo Finnigan) coupled to a MAT 253 gas source mass spectrometer (Thermo Finnigan) at the Goethe University - Senckenberg BiK-F Joint Stable Isotope Facility (Frankfurt).

20   USGS 24 and IAEA-CH-7 standard materials were analyzed on a daily basis and replicate measurements of reference materials and samples indicate uncertainty of < 0.2 ‰ for measured $\delta^{13}C_{TOC}$ values. Total organic carbon concentrations [in %] were calculated by relating the signal size of the samples and the averaged signal size of the daily standards (USGS 24, n =8). The typical error is ~0.5 % based on mass spectrometric analysis and the maximum difference in TOC contents of replicate measurements (including weighing uncertainties) was ~7 %.

2.3 Palynological analyses

25

The palynological analysis is primarily based on revised data of 59 samples from a section between the top of the Main Seam and the top of Seam 2 (Hammer-Schiemann, 1998). For palynological processing, lignite samples were crushed to a particle size of 1 to 2 mm. All lignite and interbed samples were treated with hot 15% hydrogen peroxide (H_2O_2) and ca. 5% potassium hydroxide (KOH) for 1 to 2 h. The clastic samples were further treated with 30% hydrofluoric acid (HF) for

30   several days. HF was removed by 5 to 6 steps of decanting and diluting. All samples were sieved through a 10 μm-mesh sieve. Residues are stored in glycerine and permanent glycerine jelly slides were made. To obtain a representative dataset, at

least 300 individual grains of pollen and spores were counted per sample at ×400 magnification (data in Supplementary Information table S3). The palynomorphs were mainly identified on the basis of systematic-taxonomic studies Thomson and Pflug (1953), Krutzsch (1970), Thiele-Pfeiffer (1988), Nickel (1996), Hammer-Schiemann (1998) and Lenz (2005). The simplified pollen diagram shows the abundance of the most important palynomorphs in percentages. Pollen and spores were

5 calculated to 100% whereas dinoflagellate cysts (*Apectodinium* sp.) and charcoal particles larger than *c*. 10 μm were added as additional percentages (in percent of the total pollen sum).

3 Results and Discussion

3.1 The CIE in the basal Schöningen Formation

The total organic carbon content across the analyzed section ranges from ~0.2 % to 69 % and correlates with lithology
10 generally with TOC contents >50 % in the lignite seams and <10 % in the clastic interbed (Fig. 2a). Carbon isotope ratios of bulk organic matter range from -25.1 ‰ to -28.3 ‰ (Fig. 2b). In the basal part (0 to 2.9 m) of the section $\delta^{13}C_{TOC}$ varies between -25.7 ‰ and -27.4 ‰ (average $\delta^{13}C_{TOC}$ = -26.76 ±0.46 ‰, n=26). At 3.0 m of section, $\delta^{13}C_{TOC}$ abruptly decreases to values as low as -28.3 ‰ and remains low within the next 0.7 m (average $\delta^{13}C_{TOC}$ = -28.02 ±0.19 ‰, n=8). At 3.9 m of section, $\delta^{13}C_{TOC}$ values increase to 26.95 ±0.16 ‰ (n=37) and remain constant (-26.5 ‰ to -27.3 ‰) for the next 6.5 m
15 before they decrease again to -28.1 ‰ (at 10.6 m) and reach values as low as -28.3 ‰ (at 12.4 m). Between 12.4 m and 12.9 m $\delta^{13}C_{TOC}$ increases to a value of -26.2 ‰ (at 12.9 m) and attains an average of $\delta^{13}C_{TOC}$ = -26.20 ±0.43 ‰ (n=18, 12.9 to 15.8 m), very similar to the pre-excursion $\delta^{13}C_{TOC}$ values in the 0-2.9 m part of the section.

Overall, the $\delta^{13}C_{TOC}$ data show four conspicuous shifts across the record (Fig. 2b): The basal shift at 3.0 m of section to lower $\delta^{13}C_{TOC}$ values ($\Delta\delta^{13}C_{TOC, single samples at \sim 3m}$ = -1.7 ‰) and the uppermost gradual increase between 12.4 m and 12.9 m
20 back to higher ($\Delta\delta^{13}C_{TOC, 12.4m-12.9m}$ = +2.1 ‰) $\delta^{13}C_{TOC}$ values occur within individual lignite seams and thus are both independent of major lithological changes (Fig. 2). In contrast, the $\delta^{13}C_{TOC}$ shifts at 3.9 m ($\Delta\delta^{13}C_{TOC, 3.9m}$ = +0.9) and between 10.3-10.6 m ($\Delta\delta^{13}C_{TOC, 10.6m}$ = -1.3 ‰) correlate with lithological changes. Most importantly, the remarkably stable $\delta^{13}C_{TOC}$ values in the central part of the section (3.9 to 10.6 m) are restricted to the clastic Interbed 2 deposited under marine conditions. Omitting these marine samples (with %TOC <10 %), indicates that the low $\delta^{13}C_{TOC}$ values smoothly tie between
25 Seam 1 and Seam 2 with an average value of -27.68 ±0.43 ‰, whereas $\delta^{13}C_{TOC}$ values in the shallow marine sediments (Interbed 2) are ~0.7 ‰ higher. Higher $\delta^{13}C_{TOC}$ values in the clastic interbed may result from mixing of different carbon sources (marine and fluvial material) compared to the local deposits of the peat mire. The low $\delta^{13}C_{TOC}$ values at the base of Interbed 2 (3 samples with ~-28 ‰) may indicate reworking of the underlying peat deposits which is supported by scattered lignite material in the sediments.
30 As a consequence, we consider the excursion in $\delta^{13}C_{TOC}$ within the lignite seams and thus independent of lithological changes to demark the onset and termination of the PETM-related CIE as it occurs in the two seams surrounding the clastic

interbed that includes the prominent *Apectodinium* acme (Riegel et al., 2012). In particular the abrupt decrease ($\Delta\delta^{13}C_{TOC}$ = -1.7 ‰ within 0.08 m of section (2.94 to 3.02 m)), but the more gradual increase of $\delta^{13}C_{TOC}$ values ($\Delta\delta^{13}C_{TOC}$ = +2.1 ‰ within 0.52 m of section (12.41 to 12.93 m)) in our record resembles the characteristic PETM-related carbon isotope excursion with a discernable onset and recovery of the CIE (c.f. McInerney and Wing, 2011). Detailed biogeochemical

5   investigations of Seam 1 in a nearby section from Schöningen also showed a gradual depletion in $\delta^{13}C_{TOC}$ as well as in mid- and long-chain *n*-alkanes at the top of Seam 1 (Inglis et al., 2015, 2017). Moreover, the absolute %TOC and $\delta^{13}C_{TOC}$ values published by (Inglis et al., 2015) are in very good agreement with our newly derived data and reveal a statistically significant (single-tailed t-test p< 0.000003) negative shift in $\delta^{13}C_{TOC}$ values at the top of Seam 1 with $\Delta\delta^{13}C_{TOC}$ = ~ -1.0 ‰ (from average $\delta^{13}C_{TOC}$ = -26.53 ±0.30 ‰ to $\delta^{13}C_{TOC}$ = -27.52 ±0.09 ‰) (Fig. 3a).

10   The CIE in Schöningen comprises the top of Seam 1, Interbed 2 and base of Seam 2, in total ~10 m of section, which makes it one of the most extensive PETM records in Central Europe. Given the total duration of the CIE during the PETM of ca. 120-220 ka our sample resolution of ~ 13 cm would translate into a temporal resolution of 1.6-2.9 ka. Based on previous age constraints, Brandes et al. (2012) independently deduced high sedimentation rates of 60-80 m/Ma for the lower part of the Schöningen Formation. Thus, our CIE of 10 m would translate into a duration of 125-167 ka, which agrees well with

15   reported PETM durations of 120-220 ka (McInerney and Wing, 2011; Röhl et al., 2007) despite the associated uncertainty of different deposition rates in the different analyzed lithologies (Trampush and Hajek, 2017).

3.2 The magnitude of the CIE in European lignite records

Even though the magnitudes of the CIE vary widely among proxy records (c.f. McInerney and Wing, 2011; Sluijs and Dickens, 2012), the CIE in the Schöningen record is small given the generally large CIE in bulk organic carbon in terrestrial

20   settings (e.g. bulk soil organic matter mean -3.5 ±0.6‰ (n=14); McInerney and Wing (2011)). Terrestrial CIEs are commonly enhanced by ~1-3‰ compared to those inferred from marine organic matter (typically in the range of -2 to -3‰; e.g. Cramer and Kent (2005); McInerney and Wing (2011); Sluijs and Dickens (2012)). Thus, it may be questioned whether the reduced CIE at Schöningen is unique due to local conditions and can be actually related to the PETM or whether it is an general feature of the mid latitudinal European near-coastal environments. We therefore compared our $\delta^{13}C_{TOC}$ record and

25   the adjacent record of Inglis et al. (2015) with published peat mire records along the paleo-North Sea coast line (Fig. 1), namely the Cobham Lignite (UK) (Collinson et al., 2003, 2009; Pancost et al., 2007) and the Vasterival section (France) (Garel et al., 2013; Storme et al., 2012). All three lignite deposits share characteristic features (Table 1; Fig. 3 and Fig. 4):

   (1) absolute $\delta^{13}C_{TOC}$ values as well as the range in $\delta^{13}C_{TOC}$ values (~3.2 ‰) are very similar;

   (2) all three records attain similar minimum $\delta^{13}C_{TOC}$ values during the CIE (-27.5 ‰ to -28.8 ‰), averaging at 28.05

30   ±0.5 ‰ (Fig. 4);

   (3) the magnitude of changes in $\delta^{13}C_{TOC}$ at the onset of the CIE (calculated as the difference between the last pre-CIE value and the first CIE value) ranges between -1.4 to -1.8 ‰ (Fig. 3);

(4) reported magnitudes of the CIE in bulk organic matter calculated as the difference between the mean pre-CIE and the mean CIE values range from 0.9 to 1.6 ‰. The CIEs, calculated as the difference between the mean pre-CIE values and the most negative value during CIE (following McInerney and Wing (2011), c.f. Fig. 4) yields magnitudes of 1.1 to 2.3 ‰ (Table 1).

5   Overall, the comparison of these geographically adjacent deposits shows that all reported CIE magnitudes of lignite records along the paleo-North Sea are dampened compared to purely continental terrestrial archives but yield a very consistent and thus robust signal (Fig. 4). Depending on the definition of the CIE, the average magnitude is 1.27 ±0.29 ‰ ("mean-mean") or 1.74 ±0.46 ‰. ("mean-most negative value") and the average decrease of $\delta^{13}C_{TOC}$ values at the onset of the CIE is -1.39 ±0.43 ‰ (Table. 1).

10 There are multiple possibilities to explain the dampened magnitude in these deposits such as mixing and dilution of the input signal, occurrence of local signal perturbation (e.g. due to vegetation changes), or differential degradation/preservation of organic matter during the climatic perturbation.

Mixing and dilution of the PETM signal in the Schöningen estuarine depositional context, where multiple flooding and thus reworking events may have occurred, appears unlikely as the observed CIE onset is sharp (i.e. between 2 samples within 8

15 cm) and within a lignite seam where no mixing of sediment occurred. The organic matter of the original peat likely resulted from an ombrotrophic (rain-fed) peat mire (consisting mostly of mosses, ferns, and associated hardwood mire forest, see section 3.3) (Inglis et al., 2015; Riegel et al., 2012) and has to be regarded as autochthonous with transport (if any) only on very short distances, likely meters.

It is possible that the reduced CIE magnitude is a local signal derived by changes in plant communities during the PETM.

20 For instance, variable angiosperm : gymnosperm ratios caused significant variations in the recovered $\delta^{13}C_{TOC}$ values of Miocene lignites from Austria (Bechtel et al., 2003) and a similar scenario appears possible during the PETM. However, in our pollen record we do not observe particular changes from angiosperms to gymnosperms in conjunction with the CIE. Similar to the Schöningen record, the Cobham palynological record lacks major changes in the paleofloral community along with the CIE (Collinson et al., 2003, 2009). Collinson et al. (2009) found only subtle vegetation changes across the PETM in

25 the Cobham lignites and primarily attributed these to changes in the local fire regime. Collinson et al. (2003) also discussed that the carbon isotope variability in the Cobham Lignite may have been caused by local changes in the depositional environment, the preservation states, or the plant communities, but at the same time excluded those mechanisms because the major shift in the carbon isotope values occurred without any major lithological or floral changes. Moreover, marine sediments from the paleo-North Sea exhibit an enhanced CIE of 6-8 ‰ that has been explained by increased terrigenous

30 input (Heilmann-Clausen and Schmitz, 2000; Schmitz et al., 2004; Sluijs and Dickens, 2012). Land plant derived $\delta^{13}C$ values of n-alkanes from two sections of the paleo-North Sea (Denmark) record a decrease of 4–7 ‰ (Schoon et al., 2015), clearly showing that the PETM affected the biosphere around the paleo-North Sea in terms of recording the CIE. However, Schoon et al. (2015) also noted that the differences in the CIE likely arose from local differences in the plant communities or

precipitation patterns. Taken together, we think that a local change in vegetation, altering the carbon isotope "input signal" to the peat mires, is unlikely to account for the reduced CIE in the Schöningen lignites.

An alternative scenario is differential degradation/preservation of organic matter in the Schöningen peat mires during the PETM. Carbon isotope discrimination between litter input and stored (soil) organic matter during degradation/decomposition

5   is governed by fractionation processes during metabolism (typically enriching the residual carbon stock in ^{13}C) and the selective utilization of compounds (with differing $\delta^{13}C$ values) (e.g. Santruckova et al., 2000). The latter process apparently dominates and can either enhance or suppress a metabolism-related fractionation signal (Santruckova et al., 2000). Minor warming of ~1°C can cause significant increases in carbon respiration rates (on average 52 % in spring to 60 % in summer; Dorrepaal et al., 2009) in modern high-latitude peatlands. Contemporaneous to the increased respiration rates, an increase in

10   the carbon isotope ratios of the respired CO_2 has been interpreted as a shift towards respiration of less ^{13}C-depleted carbon stocks, likely due to a change in microbial communities. Even though the paleoenvironmental setting of the Paleogene peat mire clearly differs from the modern high-latitude mires (Dorrepaal et al., 2009), it seems likely that PETM-related warming generally affected the mire by increasing the respiration rates and causing changes in the microbial community, which could have resulted in specific changes in the $\delta^{13}C$ values of the respired and residual carbon stocks in peatlands. Indeed, Pancost

15   et al. (2007) attributed the shift in $\delta^{13}C$ values of hopanes, a biomarker derived from bacteria, in the Cobham Lignite Bed to an increase in the population of methanotrophic bacteria and, possibly, decreased heterotrophic biomass in this peatland during the PETM, thus, documenting a major shift in the microbial community during the PETM. Hopane data from Schöningen have been interpreted in terms of a generally mixed methanotrophic and heterotrophic bacterial population (Inglis et al., 2015). The decreasing trend in $\delta^{13}C$ values of hopanes at the top of Seam 1 may indicate slight changes in the

20   bacterial communities associated with the PETM, even though no significant warming trend (based on branched-GDGTs) was detected here (Inglis et al., 2015, 2017). Thus, higher-than-expected $\delta^{13}C_{TOC}$ values during the CIE relative to pre-CIE values could result from enhanced microbial degradation processes and changed microbial communities that decompose more ^{13}C-depleted recalcitrant matter during the PETM. Generally enhanced respiration rates and changes in the microbial communities due to warming (and wetting) are also likely to appear on a regional scale and are thus, consistent with our

25   finding of generally reduced CIEs in peat mires along the paleo-North Sea.

3.3 Environmental changes in the Schöningen peat mire associated with the PETM

The repeated change from open estuary/marine to meandering river/peat mire environments is characteristic for the Schöningen Formation and continues even into the middle Eocene Helmstedt Formation (Fig. 1b) (Riegel et al., 2012, 2015). However, identification of the PETM-related CIE now allows a detailed assessment of microfloral changes directly

30   associated with climatic changes during the PETM. We extended our palynological data set down-section to the underlying Interbed 1 and Main Seam in order to disentangle effects of transgressions/regressions in the coastal setting which were

governed by an interplay of eustatic sea level changes, withdrawal of salt towards the salt wall and/or changes in precipitation and subsequent runoff from the direct effects of the PETM climate perturbation.

During the late Paleocene and early Eocene mire forests typical for coastal areas along the edge of the paleo-North Sea basin, existed in the area of Schöningen (e.g. Allen, 1982; Collinson et al., 2009). As inferred from pollen records they consisted

5   essentially of wet swamp forests dominated by Nyssaceae and Cupressaceae s.l. and dryer hardwood mire and background forests characterized by Fagaceae and Myricaceae/Betulaceae (Riegel et al., 2012, 2015). Three groups of palynomorphs can be distinguished (Fig. 5): (1) taxa that occur throughout the entire succession but with frequency maxima in the interbeds 1 and 2 such as pollen of Cupressaceae s.l. (*Inaperturopollenites* spp., *Cupressacidites* sp.), Fagaceae resp. Leguminosae (*Tricolpopollenites liblarensis*), Fagaceae (*Tricolporopollenites cingulum*) or Myricaceae/Betulaceae (*Triporopollenites*

10 *robustus* group), (2) taxa that are especially abundant in some of the interbed-lignite seam transitions, such as the juglandaceous pollen *Plicapollis pseudoexcelsus* (Main Seam/Interbed 1 and Interbed 1/Seam 1) and *Thomsonipollenites magnificus* (Interdbed 2/ Seam 2 and to a lesser extent Main Seam/Interbed 1) (the latter with unknown botanical affinity), and (3) taxa that are strictly confined to lignite seams, e.g. spores of peat mosses (Spagnaceae) or spores of polypodiaceaous ferns.

15 The mostly fagaceous pollen *T. liblarensis* and *T. cingulum* appear to be essentially confined to the CIE (9-14 m in Fig. 5). However, when compared with the older part of the succession (0-6 m in Fig. 5), these taxa appear more frequently in the marine interbeds. Presumably, with the rise of the sea level the respective forests shifted landward and the small wind-transported fagaceous pollen became enriched in the interbeds at this site. For the same reason, pollen of the Cupressaceae s.l. indicative of a swamp forest, occur more frequently in the marine interbeds. Myricaceae/Betulaceae dominated forests as

20 represented by *T. robustus*-group pollen are considered to have grown on better drained, remote mire areas and are therefore less affected by sea-level fluctuations (Riegel et al. 2012).

Floral successions at marine interbed/lignite transitions at Schöningen differ significantly from those of the middle Eocene Helmstedt Formation in nearly lacking pollen of the tropical mangrove elements *Rhizophora*, *Avicennia*, *Nypa* and *Psilodiporites* of unknown botanical affinity (Lenz, 2005; Lenz and Riegel, 2001; Riegel et al., 2012, 2015; this study).

25 Instead, transitions at Schöningen are characterized by *Thomsonipollis magnificus*, *Pistillipollenites mcgregorii* (Fig. 5). *Plicapollis pseudoexcelsus*, and *Pompeckjoidaepollenites subhercynicus*, the latter two being also known from the middle Eocene of the Helmstedt Formation as back mangrove elements (Lenz and Riegel, 2001). The absence of tropical mangrove elements, especially *Nypa*, has been interpreted as indicating extratropical conditions during the deposition of the Schöningen Formation in contrast to the true tropical conditions during the middle Eocene (Helmstedt Formation) (Riegel et

30 al., 2012).

Spores of Sphagnaceae (peat mosses) and polypodiaceous ferns are typical lignite related elements throughout much of the Schöningen Formation and often dominate the palynological assemblages (Inglis et al., 2015; Riegel and Wilde, 2016; Riegel et al., 2012). The frequent and close association of these spores (*Sphagnumsporites spp., Distancorisporis sp., Tripunctisporis sp., Laevigatosporites spp.*) with charcoal horizons is characteristic for Seam 1 and Seam 2 and has been

interpreted as the secondary vegetation succeeding forest fires (Hammer-Schiemann, 1998; Inglis et al., 2015; Riegel et al., 2012; Robson et al., 2015). *Sphagnum* spores sharply decline at the top of Seam 1 and reappear with considerable delay in Seam 2 (above 13.2 m in Fig. 5). This *Sphagnum*-free interval coincides exactly with the range of the detected CIE and could potentially reflect a response to PETM warming. However, a similar distribution pattern of *Sphagnum*-spores has been observed in the lower part of Seam 1 (Fig. 5 and Inglis et al. (2015)) as well as in the Main Seam (Hammer-Schiemann 1998), suggesting that the return of peat mosses is typical for post-fire successions of peat-forming mires following marine incursions at Schöningen. Even though Storme et al. (2012) reported dry/wet cycling across the late Paleocene and early Eocene with rather dry conditions during the main part of the CIE at Vasterival (France), we exclude overall drying as the cause of suppressed proliferation of Sphagnaceae at Schöningen during the PETM. Similar to the Cobham Lignite (Collinson et al., 2003), waterlogged conditions are indicated at the top of Seam 1 by the presence of freshwater phytoplankton and confirmed by multiple biomarker analyses (Inglis et al., 2015). Furthermore, regional proxy records indicate increased terrestrial runoff (Bornemann et al., 2014; Heilmann-Clausen and Schmitz, 2000; Schmitz and Pujalte, 2003), consistent with climate model outputs which show generally increased but also more variable rainfall during the PETM (e.g. Carmichael et al., 2016, 2017). Therefore, either increased nutrient inputs to the mire or climatic changes during the PETM may have restrained proliferation of Sphagnaceae and promoted the spread of higher plants such as (e.g. Cupressaceae s.l. and parent plants of *T. cingulum* and *T. liblarensis*).

In summary, our palynological data indicate only minor changes of plant taxa during the PETM. Long-term environmental records are needed to identify whether plant community changes were forced by (1) lithological/environmental changes, (2) PETM related climate changes, or (3) a combination of both. Hitherto, changes in plant communities seem to follow natural successions at marine-terrestrial interfaces rather than climatic patterns.

3.4 Schöningen in relation to other European lignite records

In the Cobham Lignite record minor qualitative changes among plant species contrast major changes in the composition of the plant community across the PETM onset, which includes the disappearance of ferns and the increase in cupressaceous conifers (Collinson et al., 2003, 2009). This is remarkably similar to Schöningen, where the disappearance of ferns prior the onset of the CIE is followed by a similarly high but more fluctuating occurrence of Cupressaceae during the CIE with similarly high but more fluctuating occurrence of Cupressaceae throughout the record (Fig. 5).

Strikingly similar at both localities, Schöningen and Cobham, is the high abundance of charcoal prior to the PETM. This charcoal is in close association with abundant fern spores and is most likely derived from a secondary vegetation succeeding wildfires at the onset of the PETM (Collinson et al., 2003, 2009). At Schöningen, a high abundance of charcoal occurs in Seam 1 and Seam 2 (Riegel et al., 2012; Robson et al., 2015) with particular high charcoal contents in the upper part of Seam 1 compared to its base (Inglis et al., 2015; Robson et al., 2015). Thus, this increase in fire intensity immediately precedes our PETM-related CIE (Fig. 5). Evidence for high frequency of wildfires from Schöningen and Cobham prior to the PETM is

compatible with the hypothesis that peat burning was an important trigger for the CIE (Kurtz et al., 2003; Moore and Kurtz, 2008).

Another common characteristic of the lignite records at Schöningen, Cobham, and Vasterival is drowning of the peat mires just subsequent to the onset of the detected CIE (Collinson et al., 2003; Garel et al., 2013, this study, Brandes et al., 2012;

5 Riegel et al., 2012). A global transgressional phase (e.g. Sluijs et al., 2011) likely resulted in the deposition of the marine clastic Interbed 2 at Schöningen during much of the PETM (Fig. 2). The return of the Schöningen peat mire (Seam 2) may have been caused by a decrease of thermal expansion of the ocean and a concomitant global regression during cessation of the PETM. At the same time, increased sediment supply from the hinterland during the PETM (e.g. Bornemann et al., 2014; Heilmann-Clausen and Schmitz, 2000) filled the available accommodation space.

10 **4 Summary and Conclusion**

Carbon isotopic and palynological data from an alternating succession of lignite and clastic deposits in the basal Schöningen Formation (Germany) show characteristic features of the PETM: a negative CIE ($\Delta\delta^{13}C_{TOC}$ = -1.7 ‰) and an *Apectodinium* acme. The Schöningen Formation therefore yields an extensive (~10 m exposure of the CIE) and densely sampled (sample resolution ~13 cm resulting in a temporal resolution of ~1.6-2.9 ka) mid-latitude PETM record from the marine-terrestrial

15 interface. The identification of the PETM at Schöningen has important implications for the interpretation of paleoenvironmental changes at this site, in relation to other near-by PETM records, and to linking marine and terrestrial PETM records. Comparison with other peat mire records along the paleo-North Sea coast line (Cobham, UK; Vasterival, F) shows that the carbon isotopic composition of these lignites yields a reduced, compared to marine or other terrestrial archives, but consistent CIE with a magnitude of ~1.3 ‰. Even though each sedimentary record is a unique sequence of

20 deposition, erosion, and hiatuses that likely modify the shape or extent of the climate signal (Trampush and Hajek, 2017), consistence of the CIE magnitudes of the three lignite sites along the paleo-North Sea suggests a robust regional signal.

Paleofloral changes that are clearly related to the PETM time interval are minor and most changes follow natural successions. Only long-term environmental records appear suitable to distinguish if plant communities changed due to (1) lithological/environmental changes, (2) PETM related climate change, or (3) a combination of both. Our CIE record

25 highlights that the interval of highest fire frequency in the Schöningen Formation (Seam 1, (Robson et al., 2015)) is clearly associated with the PETM. Thus, common features of the Schöningen and the Cobham Lignite records emerge, such as a similar CIE, similar paleo-floral successions, and drowning of peat mires during the major body of the CIE. Furthermore, both records yield evidence of increased fire activity such as increased charcoal contents in combination with the appearance of ferns and peat mosses prior to the PETM. Taken together, this points to similar climatic and environmental conditions

30 along the paleo-North Sea coast during the latest Paleocene to earliest Eocene, even resulting in a similar CIE of these European wetland records.

Acknowledgements

Author contributions

W.R., V.W. and A.M. designed the study. K.M. composed the paper. K.M. and A.M. conducted the geochemical analyses and evaluated the results. W.R., V.W., and O.L. provided sample material, regional geological expertise and conducted palynological analyses. All authors edited the final version of this manuscript.

References

Ahrendt, H., Köthe, A., Lietzow, A., Marheine, D., and Ritzkowski, S.: Lithostratigraphie, Biostratigraphie und radiometrische Datierung des Unter-Eozäns von Helmstedt (SE-Niedersachsen), Zeitschrift der Deutschen Geologischen Gesellschaft, 146, 450-457, 1995.

Allen, L. O.: Palynology of the Palaeocene and early Eocene of the London Basin, Ph. D., University College London, 1982.

Bechtel, A., Gruber, W., Sachsenhofer, R. F., Gratzer, R., Lücke, A., and Püttmann, W.: Depositional environment of the Late Miocene Hausruck lignite (Alpine Foreland Basin): insights from petrography, organic geochemistry, and stable carbon isotopes, International Journal of Coal Geology, 53, 153-180, 2003.

Bornemann, A., Norris, R. D., Lyman, J. A., D'Haenens, S., Groeneveld, J., Röhl, U., Farley, K. A., and Speijer, R. P.: Persistent environmental change after the Paleocene–Eocene Thermal Maximum in the eastern North Atlantic, Earth Planet Sc Lett, 394, 70-81, 2014.

Bowen, G. J., Maibauer, B. J., Kraus, M. J., Röhl, U., Westerhold, T., Steimke, A., Gingerich, P. D., Wing, S. L., and Clyde, W. C.: Two massive, rapid releases of carbon during the onset of the Palaeocene-Eocene thermal maximum, Nature Geosci, 8, 44-47, 2015.

Brandes, C., Pollok, L., Schmidt, C., Wilde, V., and Winsemann, J.: Basin modelling of a lignite-bearing salt rim syncline: insights into rim syncline evolution and salt diapirism in NW Germany, Basin Res, 24, 699-716, 2012.

Bujak, J. P. and Brinkhuis, H.: Global warming and dinocyst changes across the Paleocene/Eocene Epoch boundary, Late Paleocene–early Eocene climatic and biotic events in the marine and terrestrial records, 1998. 277-295, 1998.

Carmichael, M. J., Inglis, G. N., Badger, M. P. S., Naafs, B. D. A., Behrooz, L., Remmelzwaal, S., Monteiro, F. M., Rohrssen, M., Farnsworth, A., Buss, H. L., Dickson, A. J., Valdes, P. J., Lunt, D. J., and Pancost, R. D.: Hydrological and

associated biogeochemical consequences of rapid global warming during the Paleocene-Eocene Thermal Maximum, Global Planet Change, 157, 114-138, 2017.

Carmichael, M. J., Lunt, D. J., Huber, M., Heinemann, M., Kiehl, J., LeGrande, A., Loptson, C. A., Roberts, C. D., Sagoo, N., Shields, C., Valdes, P. J., Winguth, A., Winguth, C., and Pancost, R. D.: A model–model and data–model comparison for

5   the early Eocene hydrological cycle, Clim. Past, 12, 455-481, 2016.

Christensen, T. R., Ekberg, A., Ström, L., Mastepanov, M., Panikov, N., Öquist, M., Svensson, B. H., Nykänen, H., Martikainen, P. J., and Oskarsson, H.: Factors controlling large scale variations in methane emissions from wetlands, Geophys Res Lett, 30, 2003.

Collinson, M., Hooker, J., and Grocke, D.: Cobham lignite bed and penecontemporaneous macrofloras of southern England:

10 A record of vegetation and fire across the Paleocene-Eocene Thermal Maximum, Special Papers-Geological Society of America, 2003. 333-350, 2003.

Collinson, M. E., Steart, D. C., Harrington, G. J., Hooker, J. J., Scott, A. C., Allen, L. O., Glasspool, I. J., and Gibbons, S. J.: Palynological evidence of vegetation dynamics in response to palaeoenvironmental change across the onset of the Paleocene-Eocene Thermal Maximum at Cobham, Southern England, Grana, 48, 38-66, 2009.

15 Cramer, B. S. and Kent, D. V.: Bolide summer: The Paleocene/Eocene thermal maximum as a response to an extraterrestrial trigger, Palaeogeography, Palaeoclimatology, Palaeoecology, 224, 144-166, 2005.

Crouch, E. M., Heilmann-Clausen, C., Brinkhuis, H., Morgans, H. E., Rogers, K. M., Egger, H., and Schmitz, B.: Global dinoflagellate event associated with the late Paleocene thermal maximum, Geology, 29, 315-318, 2001.

DeConto, R. M., Galeotti, S., Pagani, M., Tracy, D., Schaefer, K., Zhang, T., Pollard, D., and Beerling, D. J.: Past extreme

20 warming events linked to massive carbon release from thawing permafrost, Nature, 484, 87, 2012.

Dickens, G. R., O'Neil, J. R., Rea, D. K., and Owen, R. M.: Dissociation of oceanic methane hydrate as a cause of the carbon isotope excursion at the end of the Paleocene, Paleoceanography and Paleoclimatology, 10, 965-971, 1995.

Dorrepaal, E., Toet, S., van Logtestijn, R. S. P., Swart, E., van de Weg, M. J., Callaghan, T. V., and Aerts, R.: Carbon respiration from subsurface peat accelerated by climate warming in the subarctic, Nature, 460, 616, 2009.

25 Dunkley Jones, T., Lunt, D. J., Schmidt, D. N., Ridgwell, A., Sluijs, A., Valdes, P. J., and Maslin, M.: Climate model and proxy data constraints on ocean warming across the Paleocene–Eocene Thermal Maximum, Earth-Sci Rev, 125, 123-145, 2013.

Garel, S., Schnyder, J., Jacob, J., Dupuis, C., Boussafir, M., Le Milbeau, C., Storme, J.-Y., Iakovleva, A. I., Yans, J., and Baudin, F.: Paleohydrological and paleoenvironmental changes recorded in terrestrial sediments of the Paleocene–Eocene

30 boundary (Normandy, France), Palaeogeography, Palaeoclimatology, Palaeoecology, 376, 184-199, 2013.

Hammer-Schiemann, G.: Palynologische Untersuchungen zur Fazies und Ökologie der Unterflözgruppe im Tagebau Schöningen (Untereozän, Helmstedt, Bez. Braunschweig), 1998. Univ. Göttingen, 1998.

Heilmann-Clausen, C., Nielsen, O. B., and Gersner, F.: Lithostratigraphy and depositional environments in the Upper Paleocene and Eocene of Denmark, Bulletin of the Geological Society of Denmark, 33, 287-323, 1985.

Heilmann-Clausen, C. and Schmitz, B.: The late Paleocene thermal maximum δ^{13}C excursion in Denmark?, Gff, 122, 70-70, 2000.

Higgins, J. A. and Schrag, D. P.: Beyond methane: Towards a theory for the Paleocene–Eocene Thermal Maximum, Earth Planet Sc Lett, 245, 523-537, 2006.

5 Iakovleva, A. I., Brinkhuis, H., and Cavagnetto, C.: Late Palaeocene–Early Eocene dinoflagellate cysts from the Turgay Strait, Kazakhstan; correlations across ancient seaways, Palaeogeography, Palaeoclimatology, Palaeoecology, 172, 243-268, 2001.

Inglis, G. N., Collinson, M. E., Riegel, W., Wilde, V., Farnsworth, A., Lunt, D. J., Valdes, P., Robson, B. E., Scott, A. C., Lenz, O. K., Naafs, B. D. A., and Pancost, R. D.: Mid-latitude continental temperatures through the early Eocene in western
10 Europe, Earth Planet Sc Lett, 460, 86-96, 2017.

Inglis, G. N., Collinson, M. E., Riegel, W., Wilde, V., Robson, B. E., Lenz, O. K., and Pancost, R. D.: Ecological and biogeochemical change in an early Paleogene peat-forming environment: Linking biomarkers and palynology, Palaeogeography, Palaeoclimatology, Palaeoecology, 438, 245-255, 2015.

IPCC: Climate change 2014: synthesis report. Core Writing Team, R. K. P. a. L. A. M. e. (Ed.), IPCC Geneva, Switzerland,
15 2014.

Kennett, J. P. and Stott, L. D.: Abrupt deep-sea warming, palaeoceanographic changes and benthic extinctions at the end of the Palaeocene, Nature, 353, 225, 1991.

Kent, D. V., Cramer, B. S., Lanci, L., Wang, D., Wright, J. D., and Van der Voo, R.: A case for a comet impact trigger for the Paleocene/Eocene thermal maximum and carbon isotope excursion, Earth Planet Sc Lett, 211, 13-26, 2003.

20 Kirschke, S., Bousquet, P., Ciais, P., Saunois, M., Canadell, J. G., Dlugokencky, E. J., Bergamaschi, P., Bergmann, D., Blake, D. R., Bruhwiler, L., Cameron-Smith, P., Castaldi, S., Chevallier, F., Feng, L., Fraser, A., Heimann, M., Hodson, E. L., Houweling, S., Josse, B., Fraser, P. J., Krummel, P. B., Lamarque, J.-F., Langenfelds, R. L., Le Quéré, C., Naik, V., O'Doherty, S., Palmer, P. I., Pison, I., Plummer, D., Poulter, B., Prinn, R. G., Rigby, M., Ringeval, B., Santini, M., Schmidt, M., Shindell, D. T., Simpson, I. J., Spahni, R., Steele, L. P., Strode, S. A., Sudo, K., Szopa, S., van der Werf, G. R.,
25 Voulgarakis, A., van Weele, M., Weiss, R. F., Williams, J. E., and Zeng, G.: Three decades of global methane sources and sinks, Nat Geosci, 6, 813, 2013.

Koch, P. L., Zachos, J. C., and Gingerich, P. D.: Correlation between isotope records in marine and continental carbon reservoirs near the Palaeocene/Eocene boundary, Nature, 358, 319-322, 1992.

Köthe, A.: Dinozysten-Zonierung im Tertiär Norddeutschlands, Revue Paléobiologie, 22, 895-923, 2003.

30 Krutzsch, W.: Die stratigraphisch verwertbaren Sporen-und Pollenformen des mitteleuropäischen Alttertiärs, Jb. Geol, 3, 309-379, 1970.

Kurtz, A., Kump, L., Arthur, M., Zachos, J., and Paytan, A.: Early Cenozoic decoupling of the global carbon and sulfur cycles, Paleoceanography, 18, 2003.

Lenz, O. K.: Palynologie und Paläoökologie eines Küstenmoores aus dem Mittleren Eozän Mitteleuropas-Die Wulfersdorfer Flözgruppe aus dem Tagebau Helmstedt, Niedersachsen, Palaeontographica Abteilung B, 271, 1-157, 2005.

Lenz, O. K. and Riegel, W.: Isopollen maps as a tool for the reconstruction of a coastal swamp from the middle Eocene at Helmstedt (northern Germany), Facies, 45, 177-194, 2001.

5   Lyons, S. L., Baczynski, A. A., Babila, T. L., Bralower, T. J., Hajek, E. A., Kump, L. R., Polites, E. G., Self-Trail, J. M., Trampush, S. M., and Vornlocher, J. R.: Palaeocene–Eocene Thermal Maximum prolonged by fossil carbon oxidation, Nat Geosci, 12, 54, 2019.

Magioncalda, R., Dupuis, C., Smith, T., Steurbaut, E., and Gingerich, P. D.: Paleocene-Eocene carbon isotope excursion in organic carbon and pedogenic carbonate: Direct comparison in a continental stratigraphic section, Geology, 32, 553-556,

10   2004.

McInerney, F. A. and Wing, S. L.: The Paleocene-Eocene Thermal Maximum: A Perturbation of Carbon Cycle, Climate, and Biosphere with Implications for the Future, Annu Rev Earth Pl Sc, 39, 489-516, 2011.

Moore, E. A. and Kurtz, A. C.: Black carbon in Paleocene–Eocene boundary sediments: A test of biomass combustion as the PETM trigger, Palaeogeography, Palaeoclimatology, Palaeoecology, 267, 147-152, 2008.

15   Nickel, B.: Die mitteleozäne Mikroflora von Eckfeld bei Manderscheid/Eifel, 18, 1-121, 1996.

Osman, A., Pollok, L., Brandes, C., and Winsemann, J.: Sequence stratigraphy of a Paleogene coal bearing rim syncline: interplay of salt dynamics and sea-level changes, Schöningen, Germany, Basin Res, 25, 675-708, 2013.

Pancost, R. D., Steart, D. S., Handley, L., Collinson, M. E., Hooker, J. J., Scott, A. C., Grassineau, N. V., and Glasspool, I. J.: Increased terrestrial methane cycling at the Palaeocene–Eocene thermal maximum, Nature, 449, 332, 2007.

20   Raghoebarsing, A. A., Smolders, A. J. P., Schmid, M. C., Rijpstra, W. I. C., Wolters-Arts, M., Derksen, J., Jetten, M. S. M., Schouten, S., Sinninghe Damsté, J. S., Lamers, L. P. M., Roelofs, J. G. M., Op den Camp, H. J. M., and Strous, M.: Methanotrophic symbionts provide carbon for photosynthesis in peat bogs, Nature, 436, 1153, 2005.

Riegel, W., Lenz, O. K., and Wilde, V.: From open estuary to meandering river in a greenhouse world: an ecological case study from the middle Eocene of Helmstedt, northern Germany, Palaios, 30, 304-326, 2015.

25   Riegel, W. and Wilde, V.: An early Eocene Sphagnum bog at Schöningen, northern Germany, International Journal of Coal Geology, 159, 57-70, 2016.

Riegel, W., Wilde, V., and Lenz, O. K.: The early Eocene of Schöningen (N-Germany)–an interim report, Austrian Journal of Earth Sciences, 105, 88-109, 2012.

Robson, B. E., Collinson, M. E., Riegel, W., Wilde, V., Scott, A. C., and Pancost, R. D.: Early Paleogene wildfires in peat-

30   forming environments at Schöningen, Germany, Palaeogeography, Palaeoclimatology, Palaeoecology, 437, 53-62, 2015.

Röhl, U., Westerhold, T., Bralower, T. J., and Zachos, J. C.: On the duration of the Paleocene-Eocene thermal maximum (PETM), Geochemistry, Geophysics, Geosystems, 8, 2007.

Rumpel, C., Amiraslani, F., Koutika, L.-S., Smith, P., Whitehead, D., and Wollenberg, E.: Put more carbon in soils to meet Paris climate pledges, Nature, 564, 32-34, 2018.

Santruckova, H., Bird, M., Frouz, J., Sustr, V., and Tajovsky, K.: Natural abundance of 13C in leaf litter as related to feeding activity of soil invertebrates and microbial mineralisation, 2000. 2000.

Schmitz, B., Peucker-Ehrenbrink, B., Heilmann-Clausen, C., Åberg, G., Asaro, F., and Lee, C.-T. A.: Basaltic explosive volcanism, but no comet impact, at the Paleocene–Eocene boundary: high-resolution chemical and isotopic records from

5   Egypt, Spain and Denmark, Earth Planet Sc Lett, 225, 1-17, 2004.

Schmitz, B., and Pujalte, V.: Sea-level, humidity, and land-erosion records across the initial Eocene thermal maximum from a continental-marine transect in northern Spain, Geology, 31, 689-692, 2003.

Schoon, P. L., Heilmann-Clausen, C., Schultz, B. P., Sinninghe Damsté, J. S., and Schouten, S.: Warming and environmental changes in the eastern North Sea Basin during the Palaeocene–Eocene Thermal Maximum as revealed by biomarker lipids,

10 Org Geochem, 78, 79-88, 2015.

Sluijs, A., Bijl, P. K., Schouten, S., Röhl, U., Reichart, G.-J., and Brinkhuis, H.: Southern ocean warming, sea level and hydrological change during the Paleocene-Eocene thermal maximum, Clim Past, 7, 47-61, 2011.

Sluijs, A. and Brinkhuis, H.: A dynamic climate and ecosystem state during the Paleocene-Eocene Thermal Maximum: inferences from dinoflagellate cyst assemblages on the New Jersey Shelf, Biogeosciences, 6, 2009.

15 Sluijs, A., Brinkhuis, H., Schouten, S., Bohaty, S. M., John, C. M., Zachos, J. C., Reichart, G.-J., Sinninghe Damsté, J. S., Crouch, E. M., and Dickens, G. R.: Environmental precursors to rapid light carbon injection at the Palaeocene/Eocene boundary, Nature, 450, 1218, 2007.

Sluijs, A. and Dickens, G. R.: Assessing offsets between the δ13C of sedimentary components and the global exogenic carbon pool across early Paleogene carbon cycle perturbations, Global Biogeochem Cy, 26, 2012.

20 Sluijs, A., Schouten, S., Pagani, M., Woltering, M., Brinkhuis, H., Damsté, J. S. S., Dickens, G. R., Huber, M., Reichart, G.-J., and Stein, R.: Subtropical Arctic Ocean temperatures during the Palaeocene/Eocene thermal maximum, Nature, 441, 610-613, 2006.

Storme, J. Y., Dupuis, C., Schnyder, J., Quesnel, F., Garel, S., Iakovleva, A. I., Iacumin, P., Di Matteo, A., Sebilo, M., and Yans, J.: Cycles of humid-dry climate conditions around the P/E boundary: new stable isotope data from terrestrial organic

25 matter in Vasterival section (NW France), Terra Nova, 24, 114-122, 2012.

Svensen, H., Planke, S., Malthe-Sørenssen, A., Jamtveit, B., Myklebust, R., Rasmussen Eidem, T., and Rey, S. S.: Release of methane from a volcanic basin as a mechanism for initial Eocene global warming, Nature, 429, 542, 2004.

Thiele-Pfeiffer, H.: Die Mikroflora aus dem mitteleozänen Ölschiefer von Messel bei Darmstadt, Palaeontographica Abteilung B, 211, 1-86, 1988.

30 Thomson, P. W. and Pflug, H. D.: Pollen und Sporen des mitteleuropäischen Tertiärs, Palaeontographica Abteilung B, 94, 1-138, 1953.

Trampush, S. M. and Hajek, E. A.: Preserving proxy records in dynamic landscapes: Modeling and examples from the Paleocene-Eocene Thermal Maximum, Geology, 45, 967-970, 2017.

Climate
of the Past
Discussions
Open Access

EGU

van Hinsbergen, D. J., de Groot, L. V., van Schaik, S. J., Spakman, W., Bijl, P. K., Sluijs, A., Langereis, C. G., and Brinkhuis, H.: A paleolatitude calculator for paleoclimate studies, Plos One, 10, e0126946, 2015.

Wing, S. L., Harrington, G. J., Smith, F. A., Bloch, J. I., Boyer, D. M., and Freeman, K. H.: Transient floral change and rapid global warming at the Paleocene-Eocene boundary, Science, 310, 993-996, 2005.

5   Zachos, J. C., Wara, M. W., Bohaty, S., Delaney, M. L., Petrizzo, M. R., Brill, A., Bralower, T. J., and Premoli-Silva, I.: A transient rise in tropical sea surface temperature during the Paleocene-Eocene thermal maximum, Science, 302, 1551-1554, 2003.

Ziegler, P.: Geological Atlas of Western and Central Europe, Shell Internationale Petroleum Maatschappij BV/Geological Society of London. Elsevier, Amsterdam, 1990.

10

Figure 1: (a) Palaeogeographic map of northwestern Europe during the early Eocene (adapted from Ziegler, 1990), showing the locations of the Schöningen open cast mine (D), Cobham (UK) and Vasterival (F). (b) Schematic stratigraphy of the Schöningen
15 **area (adapted from Brandes et al., 2012).**

Figure 2: (a) Composite stratigraphic section, (b) $\delta^{13}C$ values of bulk organic matter, and (c) total organic carbon (%TOC). Lines denote lithological changes between the marine interbed and the lignite seams (brown) and changes in $\delta^{13}C$ values independent of lithological changes (red).

20

Figure 3: Comparison of mid-latitudinal wetland $\delta^{13}C_{TOC}$ records surrounding the paleo-North Sea (cf. Fig. 1): (a) Schöningen, Germany (this study (green symbols), Inglis et al. (2015) (grey symbols)), (b) Cobham, UK (Collinson et al., 2003), (c) Vasterival, France (Storme et al., 2012). Note the different stratigraphic thicknesses due to different sediment accumulation and preservation conditions in the individual depositional environments. (d) Carbon isotopic differences at the onset of the PETM.

25

Figure 4: Comparison of terrestrial carbon isotope excursions (CIE). Data from plant-derived lipids (yellow) and soil organic matter (green) are from (McInerney and Wing, 2011). Data from peat-derived bulk organic matter are compiled from new (this study) and published studies (Collinson et al., 2003; Inglis et al., 2015; Storme et al., 2012). Filled symbols represent mean values. Whereas the pre- and post-CIE values represent mean $\delta^{13}C$ values, the CIE is given as the most negative values, following
30 **(McInerney and Wing, 2011).**

Figure 5: Simplified pollen diagram, comprising the top of the Main Seam up to the top of Seam 2 showing frequency and palynological abundance changes between pre-, peak- and post-PETM intervals. The record is characterized by three palynological groups: (1) elements with frequency maxima in the clastic interbeds (representing the hinterland), (2) interbed-
35 **lignite seam transitional elements and back mangrove equivalents, and (3) elements dominating the lignite seams. Red bar indicate the carbon isotope excursion. Brown lines demark lithological changes between lignite seams and clastic interbeds.**

17

Table

Table 1: Compilation of $\delta^{13}C_{TOC}$ data sets from European lignite deposits.

Record	min. and max. $\delta^{13}C$ value of each record [‰]	$\delta^{13}C$ range [‰]	CIE onset[b] [‰]	CIE magnitude ("mean-mean")[c] [‰]	CIE magnitude ("mean-most negative")[d] [‰]	Reference
Schöningen (D)	-25.06 to -28.29	3.23	-1.66	-1.07	-1.53	this study
Schöningen (D)	-25.95 to -27.65	1.70	-0.68	-0.92	-1.11	Inglis et al., 2015
Cobham (UK)	-24.47 to -27.50	3.03	-1.40	-1.60 (-1.16)[e]	-1.97 (-1.53)[e]	Collinson et al., 2003
Vasterival (F)	-25.4 to -28.8[a]	3.4	-1.8	-1.5	-2.3	Storme et al., 2012

[a] exact data not given in the paper, manually extracted from the published figure.

[b] CIE onset is calculated as the difference between the last pre-CIE and the first CIE sample.

[c] CIE magnitude calculated as the difference between the mean pre-CIE and the mean CIE value.

[d] CIE magnitude calculated as the difference between the mean pre-CIE and the most negative value of the CIE (following McInerney and Wing (2011).

[e] CIE magnitude omitting the described increase of $\delta^{13}C_{TOC}$ at the basal part of the Cobham record (Collinson et al., 2003) and only taking the last 6 samples prior to the onset of the CIE as reference.
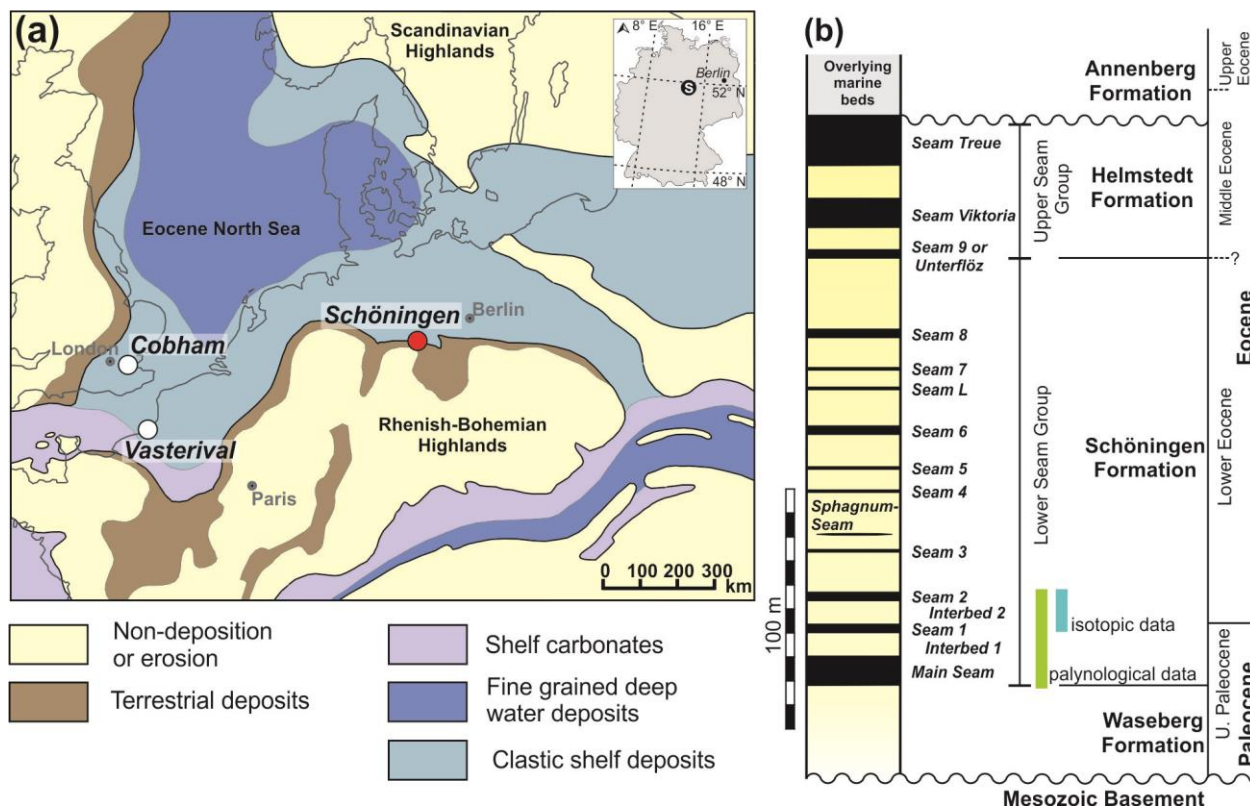
Figure 2: (a) Palaeogeographic map of northwestern Europe during the early Eocene (adapted from Ziegler, 1990), showing the locations of the Schöningen open cast mine (D), Cobham (UK) and Vasterival (F). (b) Schematic stratigraphy of the Schöningen area (adapted from Brandes et al., 2012).
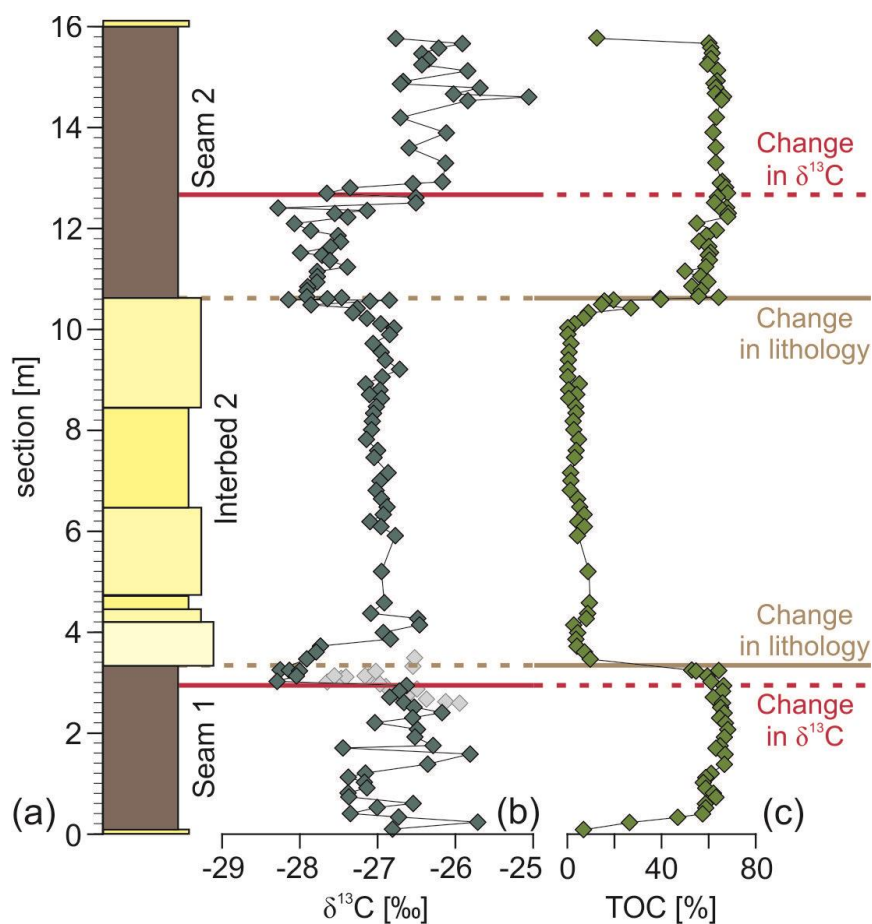
Figure 2: (a) Composite stratigraphic section, (b) δ^{13}C values of bulk organic matter, and (c) total organic carbon (%TOC). Lines denote lithological changes between the marine interbed and the lignite seams (brown) and changes in δ^{13}C values independent of lithological changes (red).
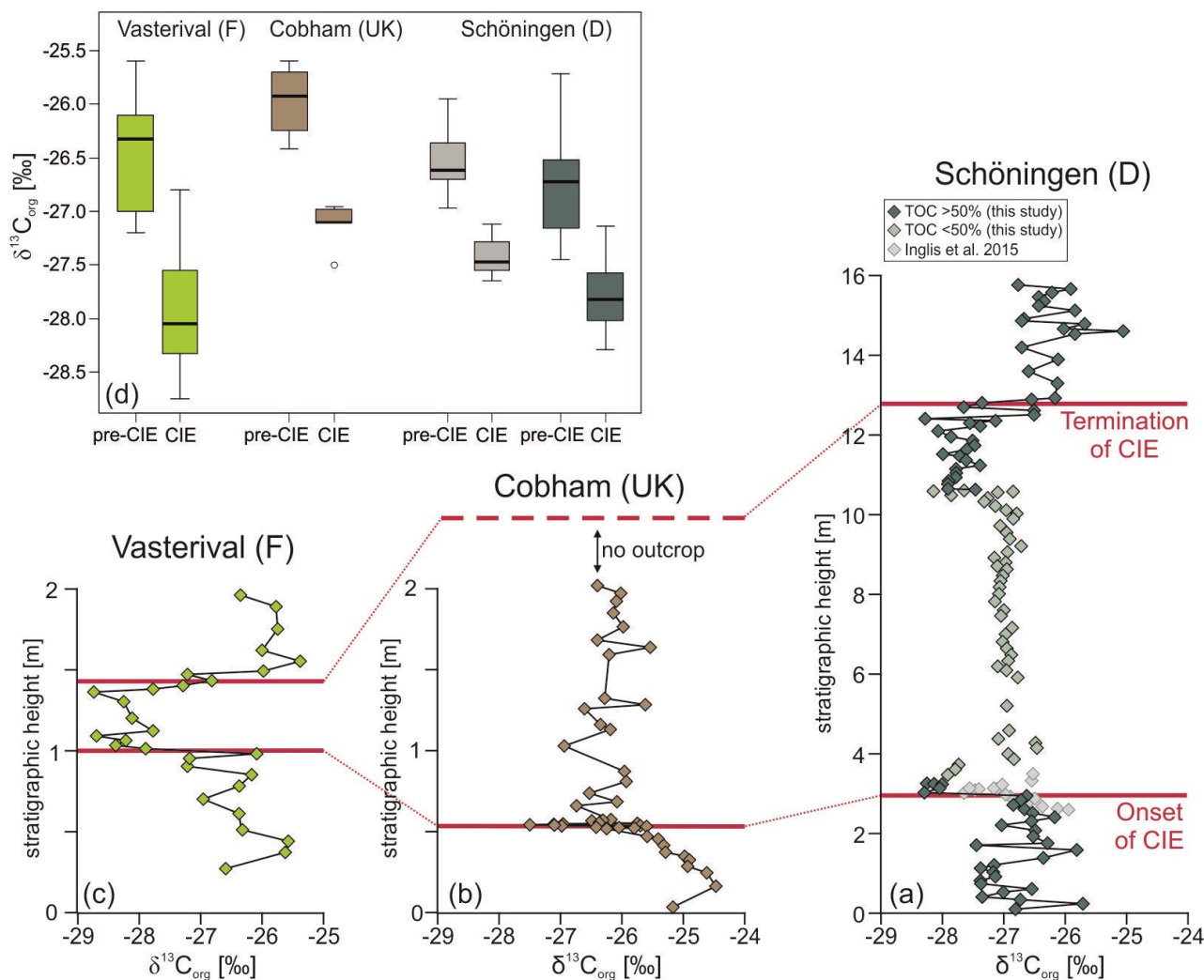
Figure 3: Comparison of mid-latitudinal wetland $\delta^{13}C_{TOC}$ records surrounding the paleo-North Sea (cf. Fig. 1): (a) Schöningen, Germany (this study (green symbols), Inglis et al. (2015) (grey symbols)), (b) Cobham, UK (Collinson et al., 2003), (c) Vasterival, France (Storme et al., 2012). Note the different stratigraphic thicknesses due to different sediment accumulation and preservation conditions in the individual depositional environments. (d) Carbon isotopic differences at the onset of the PETM.
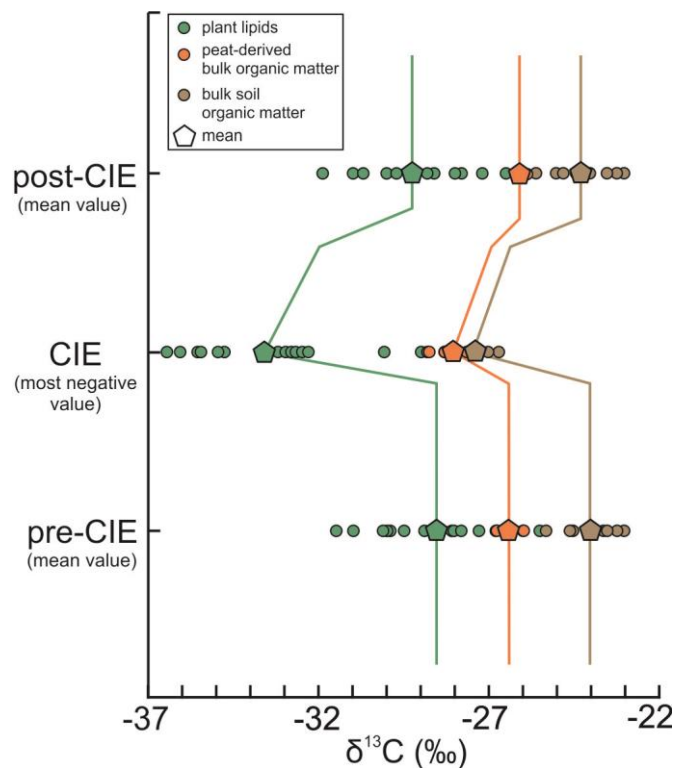
Figure 4: Comparison of terrestrial carbon isotope excursions (CIE). Data from plant-derived lipids (yellow) and soil organic matter (green) are from (McInerney and Wing, 2011). Data from peat-derived bulk organic matter are compiled from new (this study) and published studies (Collinson et al., 2003; Inglis et al., 2015; Storme et al., 2012). Filled symbols represent mean values. Whereas the pre- and post-CIE values represent mean δ^{13}C values, the CIE is given as the most negative values, following (McInerney and Wing, 2011).
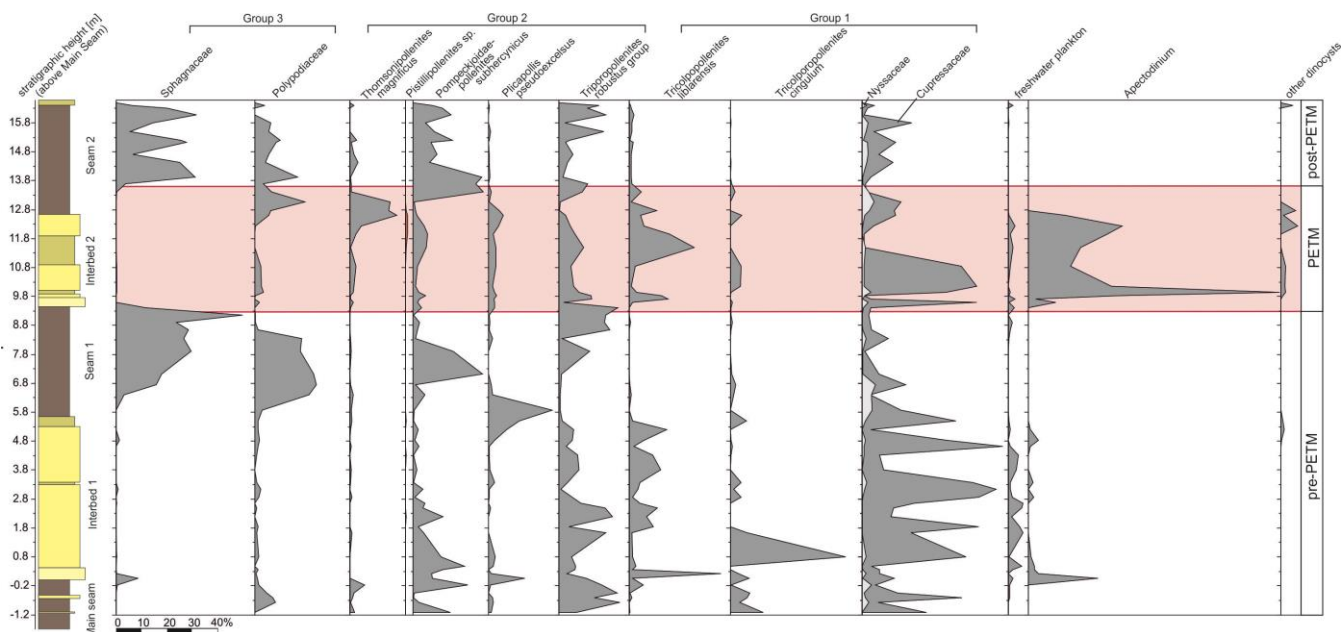
Figure 5: Simplified pollen diagram, comprising the top of the Main Seam up to the top of Seam 2 showing frequency and palynological abundance changes between pre-, peak- and post-PETM intervals. The record is characterized by three palynological groups: (1) elements with frequency maxima in the clastic interbeds (representing the hinterland), (2) interbed-lignite seam transitional elements and back mangrove equivalents, and (3) elements dominating the lignite seams. Red bar indicate the carbon isotope excursion. Brown lines demark lithological changes between lignite seams and clastic interbeds.